Interactions of 300-GeV protons with tungsten and chromium*

J. R. Florian, M. Y. Lee, J. J. Lord, J. W. Martin, and R. J. Wilkes
Department of Physics, University of Washington, Seattle, Washington 98195

R. E. Gibbs
Department of Physics, Eastern Washington State College, Cheney, Washington 99004

L. D. Kirkpatrick
Department of Physics, Montana State University, Bozeman, Montana 59715
(Received 15 September 1975)

Targets consisting of tungsten and chromium powders imbedded in nuclear emulsion were exposed to the 300-GeV proton beam at the Fermi National Accelerator Laboratory. For each event found, the number of minimum-ionizing (shower) tracks n_s and the number of heavily ionizing tracks N_h were determined, and the production angles of the shower tracks were measured. For 39 chromium events, we find $\langle n_s \rangle = 13.8 \pm 1.2$, $\langle N_h \rangle = 7.2 \pm 0.7$, and $\langle -\ln\tan(\theta_{\rm lab}/2) \rangle \equiv \langle r \rangle = 3.32 \pm 0.07$. For 51 events in tungsten, we find $\langle n_s \rangle = 18.6 \pm 1.5$, $\langle N_h \rangle = 12.9 \pm 1.2$, and $\langle r \rangle = 2.83 \pm 0.06$. The ratio $R \equiv \langle n_s \rangle / \langle n_s \rangle_p$, where $\langle n_s \rangle_p$ is the average charged multiplicity in p-p collisions, agrees with the form $R = 1/2 + \bar{\nu}/2$, where $\bar{\nu}$ is the mean number of intranuclear collisions. However, no single model adequately explains both the multiplicity and the angular distribution data.

I. INTRODUCTION

The interest in high-energy hadron collisions with nuclei has continued to grow.[1-3] This is surely due to recent improvements in experiments using identifiable nuclear targets[4-8] as well as the realization that studies involving the use of hydrogen targets can only provide us with information about the asymptotic multiparticle final state. It is the nucleus which enables us to interfere with this final state immediately after its creation, and before it reaches maturity. Hence, the nucleus becomes part of our laboratory, wherein the details of hadron dynamics can be manifested.

Initial efforts[1,2] were directed toward distinguishing two broad classes of models concerning particle production in hadron-hadron collisions. One class (one-step or incoherent models) involves those production mechanisms where the created particles become physical within the nucleus. In such a process the created particles would be free to interact with downstream nucleons and produce a cascade. Such a multiplicative process would produce a multiplicity of shower particles far in excess of that observed on hydrogen targets. The second class (two-step or coherent models) involves the production of an intermediate state of sufficient lifetime and time dilatation factor to enable it to traverse the nucleus before decaying. Thus effects of the nucleus upon the developing hadronic final state would be minimal and observed multiplicities would not differ greatly from those observed on hydrogen targets.

Experimental evidence[4,9-11] has shown that the nuclear multiplicity ratio

$$R_A = \langle n_s \rangle_A / \langle n_s \rangle_p , \tag{1}$$

where $\langle n_s \rangle_A$ is the average multiplicity of relativistic charged particles in nuclear targets of mass number A, and $\langle n_s \rangle_p$ is the proton-proton multiplicity at equal energy, is close to unity and only weakly A-dependent. Accordingly, we discuss our data on multiparticle production in tungsten ($A = 184$) and chromium ($A = 52$) only in terms of coherent production models.

II. MODELS FOR HADRON-NUCLEUS COLLISIONS

In the Landau theory[12] the volume of the intermediate state immediately formed after a collision of two hadrons is too small to contain a well-defined number of particles. The system evolves into the multiparticle final state only when it expands to a sufficiently large volume to accommodate the final number of particles. This fast expansion is relativistically hydrodynamic in character and is described by thermodynamic collective variables, such as pressure and entropy. When a proton collides with a large nucleus, the Landau model views the proton as cutting a tunnel through the nucleus. Since all this takes place during the intermediate phase of newly created hadronic matter when particle counting makes no sense, nuclear cascading is precluded. Thus the theory predicts a weak dependence of the multiplicity of created particles on the size of the struck nucleus,

$$R_A = A^{0.19}, \tag{2}$$

independent of energy.

Dar and Vary[1] use an optical model to describe the interaction of a hadron with a nucleus. The intermediate states are generated by diffractive excitation of the beam and target particles. The first collision of the beam particle with a constituent nucleon produces a fast and a slow excited state of matter. The fast one continues through the nucleus with a mean free path identical to that of the incident particle, and creates another slow excited state in each subsequent collision with a nucleon. After the fast state emerges from the nucleus, it decays into $\frac{1}{2}\langle n_s\rangle_p$ particles. Each of the slow excited states becomes $\frac{1}{2}\langle n_s\rangle_p$ particles. Therefore, if the average number of collisions of the beam particle and its excited state in a nucleus is $\bar{\nu}_A$, then

$$R_A = \tfrac{1}{2} + \tfrac{1}{2}\bar{\nu}_A . \tag{3}$$

Fishbane and Trefil[13] have also derived this result using their coherent-production model (CPM).

The energy-flux–cascade (EFC) model has been proposed by Gottfried[3] and has characteristics common to the above models. For the collective variable, he uses the energy-momentum flux of hadronic matter to describe the early evolution of a colliding system. The only input to the model is the single-particle spectrum known from proton-proton collisions. Classical equations of motion are used to extrapolate this spectrum backward in time in order to determine the stress tensor of the energy-momentum pulse formed upon collision. This pulse, formed in the initial collision of projectile with a nucleon, takes on the aspects of two hadrons, named the hard and soft hadrons. The hard hadron retains the quantum numbers and nearly all the energy E of the projectile and continues through the nucleus with the mean free path of the projectile. Every subsequent collision of the hard hadron results in very little energy loss but creates another soft hadron with energy $\sim E^{1/3}$. Each soft hadron eventually becomes the source of $\frac{1}{3}\langle n_s\rangle_p$ particles and each hard hadron becomes $\frac{2}{3}\langle n_s\rangle_p$ particles, yielding the predicted value

$$R_A = \tfrac{2}{3} + \tfrac{1}{3}\bar{\nu}_A . \tag{4}$$

The two-phase model (TPM) of Fishbane and Trefil[14] is a generalization of Gottfried's model which removes the division of the single-particle rapidity spectrum into two bulk states of matter with very different properties. They argue that any rapidity slice of the energy-momentum flux has a probability of generating upon collision an excited state of matter. This probability is proportional to the slice thickness but independent of the rapidity. The resultant prediction for R_A is identical to the prediction of Dar and Vary.

A common feature of the latter three models is the linear dependence of R_A on $\bar{\nu}_A$:

$$R_A = (1-\eta) + \eta\bar{\nu}_A , \tag{5}$$

where $\eta = \frac{1}{2}$ or $\frac{1}{3}$. While some efforts[3,13] have gone into calculating $\bar{\nu}_A$ theoretically using various ground-state nuclear densities, a more reliable method is to use the relationship[15]

$$\bar{\nu}_A = A\sigma_{pp}/\sigma_{pA} , \tag{6}$$

where σ_{pp} and σ_{pA} are the absorption (inelastic) cross sections of protons on protons and protons on nuclei, respectively. Denisov *et al.*[16] have measured σ_{pA} for various elements and energies and obtained the empirical form $\bar{\nu}_A = 0.699A^{0.309}$. This corresponds closely to calculations made by us and others[17] using a Woods-Saxon form for the nuclear density.[18]

III. EXPERIMENTAL PROCEDURE

Although the idea of loading nuclear emulsion with target materials in powder form is an old one,[19] the technique used here is new. Several 10 cm×20 cm×200 μm emulsions were prepared on glass and allowed to dry. Then a slurry was made by mixing less than one gram of powder in a beaker containing about 100 cc of water. This combination was spun by hand rapidly to distribute the metal powder uniformly in the water. The swirling mixture then was poured quickly over the emulsion plate and resulted in a fine silt coat. A second 200 μ emulsion layer was finally added and the resultant sandwich was dried. Carbon (diamond dust), chromium, silver, bismuth, and tungsten powders slurried well. The powders were of 325 mesh which yielded an average granule diameter of about 15 μ.

For this experiment, the sandwich method of loading had important advantages. Scanning was confined to a single plane and events of interest were guaranteed at least 200 μ of observable track length.

The prepared plates were exposed to the 300-GeV proton beam at the Fermi National Accelerator Laboratory[20] until a density of about 100 000 tracks per square centimeter had been obtained. Each stack of plates was oriented with its plane parallel to the beam. Thus the incident proton track along with the very forward cone of shower particles could be followed for sufficient distances to guarantee accurate angular measurements.

After development the plates were area scanned using a 55X oil-immersion objective. The signal-

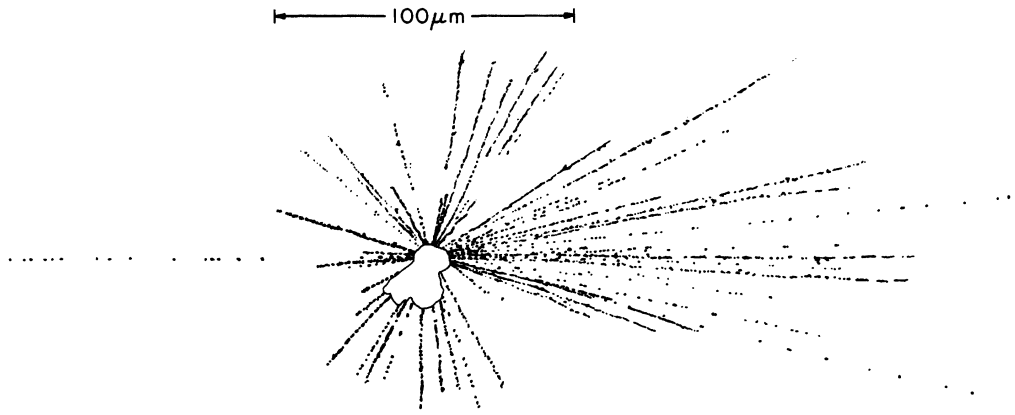

FIG. 1. Collision of a high-energy proton with a tungsten nucleus. A total of 66 tracks radiate from a common center within the tungsten granule located in the nuclear emulsion. Eighteen of the tracks were classified as shower particles.

to-noise ratio presented to the scanners was certainly less than ideal. The noise consists of a high background of minimum ionizing tracks as well as the granules themselves. An event with at least one heavily ionizing track readily catches the eye. However, we find only about 50% of white stars (events with no heavily ionizing tracks) with a multiplicity of three. White stars with a multiplicity of four or five were much easier to detect since the signal is comparable to a heavily ionizing track. Notwithstanding, we later show that the ratio R_A is not sufficiently affected by this slight scanning bias to vitiate the conclusions of this paper.

Spatial measurements using a Koristka $R4$ microscope were made on each minimum ionizing track in order to determine the production angle of each particle. These tracks were grouped according to the usual criterion:

(i) Tracks with an ionization less than 1.4 times that of a minimum ionizing track were classified as shower particles, n_s. An ionization of 1.4 minimum corresponds to a β of 0.7 or an energy of 57 MeV for pions and 375 MeV for protons.

(ii) Tracks with an ionization greater than this were classified as heavy tracks N_h. These are mainly protons knocked out or evaporated from the target nucleus.

A picture of a large tungsten event is shown in Fig. 1.

TABLE I. Summary of the multiplicity data.

Element	A	Events	$\langle n_s \rangle$	$\langle N_h \rangle$	R_A
W	184	51	18.6±1.5	12.9±1.2	2.18±0.18
Cr	52	39	13.8±1.2	7.2±0.7	1.62±0.14

IV. RESULTS

A. Multiplicity distributions

In Table I we summarize the parameters of the multiplicity distributions. The errors shown are statistical only. Figure 2 gives the multiplicity signature of each event. In Fig. 3 we present the shower particle multiplicity distribution n_s for tungsten and chromium targets. The curves drawn on the figure were obtained by Slattery[21] in his analysis of KNO-type scaling[22,23] of the charged multiplicity distributions in proton-proton interactions. The distributions were found to scale in the variable $z \equiv n_s/\langle n_s \rangle$. Although previous work[24,25] has indicated that the width of the distribution in the variable z increases with the atomic mass of the target, the statistical accuracy of the present data is not sufficient to further test this result.

Figure 4 contains the multiplicity distributions for the heavily ionizing particles N_h. In contrast

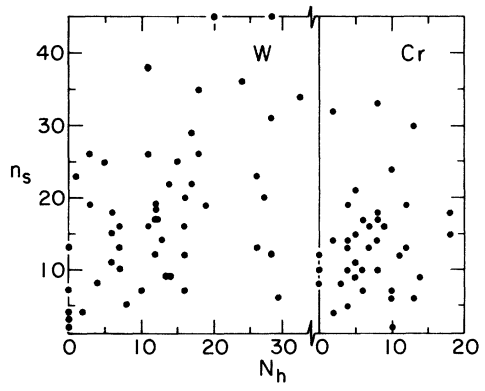

FIG. 2. A scatter plot showing the number of minimum ionizing (shower) tracks n_s and the number of heavily ionizing tracks N_h for each of the events.

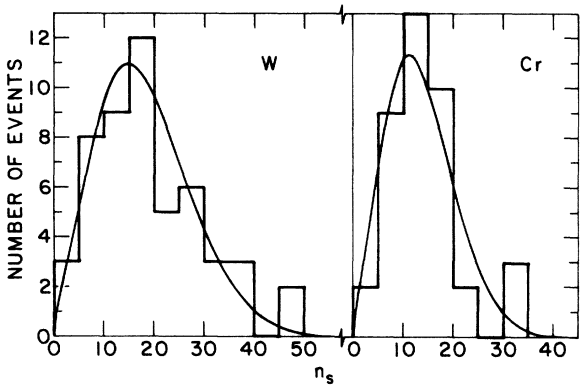

FIG. 3. Shower particle multiplicity distribution for tungsten and chromium. The solid curves were obtained by a KNO-type scaling of the charged multiplicity distribution in proton-proton interactions.

to the distribution observed in nuclear emulsion,[26,27] which is a maximum at $N_h = 0$ and falls monotonically with increasing N_h, the distributions on the pure elements show pronounced peaks at $N_h = 13$ and 8 for tungsten and chromium, respectively. The secondary peak at $N_h = 27$ in tungsten suggests that some tungsten nuclei fission. Such a process has previously been observed for gold nuclei.[28]

We next plot in Fig. 5 $\langle n_s \rangle$ against N_h for N_h bins of width five. For tungsten, the rising, linear dependence of $\langle n_s \rangle$ on N_h is reminiscent of the familiar emulsion result.[29,30] The tungsten plot has been fitted by a straight line with a χ^2 of 0.03 for 3 degrees of freedom. Otterlund[31] has fitted 1571 proton-emulsion events at 300 GeV:

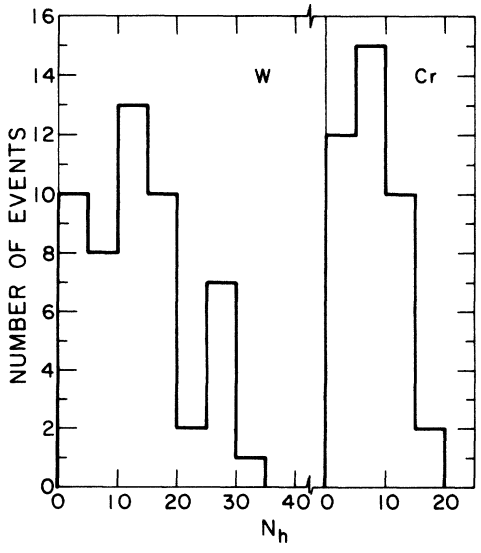

FIG. 4. Multiplicity distribution of the heavily ionizing particles emitted.

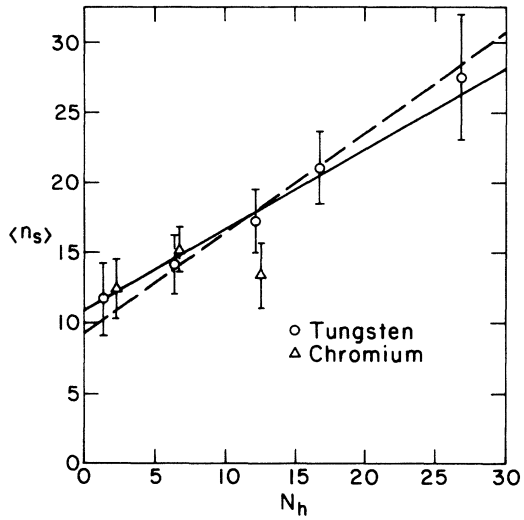

FIG. 5. Double multiplicity plot for the 51 tungsten and 39 chromium events. The solid line represents a linear fit to the tungsten data. The dashed line represents a similar fit to 300-GeV emulsion data.

$$\langle n_s \rangle = (11.0 \pm 2.4) + (0.57 \pm 0.15) N_h \text{ (tungsten)},$$
$$\langle n_s \rangle = (9.2 \pm 0.5) + (0.72 \pm 0.04) N_h \text{ (emulsion)}. \quad (7)$$

The similarity of the tungsten and emulsion data indicates that $\langle n_s \rangle$ depends chiefly on N_h rather than on the nuclear size. The apparent deviation of the chromium data from the trend of the emulsion and tungsten points may reflect some limiting phenomenon as N_h approaches the number of nuclear protons. Similar behavior has been observed in emulsion for $N_h > 20$.[10,31]

B. R vs A

Figure 6 shows the ratio R for tungsten and chromium plotted against $\bar{\nu}_A$ using Eq. (6) to calculate $\bar{\nu}_A$. We have also included emulsion and Echo Lake data.[5] The emulsion data are at 200 GeV and represent a pooling of 876 events reported by Babecki *et al.*[9] and 1068 interactions found by Hebert *et al.*[10] with 179 found in our laboratory.[26] Hebert *et al.* have also separated the emulsion data into CNO and AgBr groups. The three curves are the theoretical predictions discussed in Sec. II. The Echo Lake data tend to disagree with our data for the higher values of A. However, in that experiment the interaction vertex was not directly observed and the multiplicity was inferred from observed data via Monte Carlo corrections.

The Landau model prediction of the form $R = A^x$ with $x = 0.19$ is certainly too high. Our fit to the emulsion, chromium, and tungsten data gives $x = 0.135 \pm 0.004$ with a χ^2 per degree of freedom of 2.4/3.

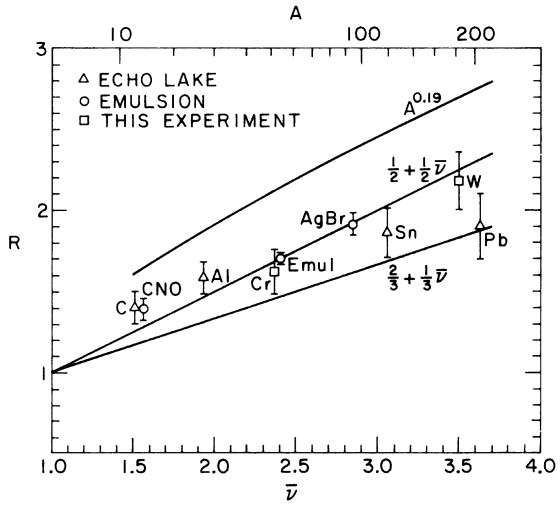

FIG. 6. Plot of the ratio R vs $\bar{\nu}$. The curves represent the predictions of the theoretical models.

The $\frac{1}{2}+\frac{1}{2}\bar{\nu}$ formula is strongly favored by the data. This conclusion, combined with the emulsion result of Eq. (7), allows the determination of the relationship between $\bar{\nu}$ and N_h,

$$\bar{\nu} = (1.16 \pm 0.12) + (0.17 \pm 0.01) N_h .$$

The major source of systematic error in this experiment is the possible scanning bias against low multiplicity white stars. In order to investigate the sensitivity of R_A to scanning bias, one may use the well-determined 200-GeV emulsion multiplicity distribution. If all $N_h = 0$, $n_s = 2$, 3 and 4 events are excluded (corresponding to zero scanning efficiency for these categories), the value of R for emulsion increases about 3%. Since our chromium and tungsten data contain white stars in this n_s range, our scanning efficiency for these white stars is greater than zero. Furthermore, the proportion of white stars present in our data should be smaller than in the emulsion data since about 40% of white stars in emulsion are hydrogen events. Thus our overestimate of R_A should be considerably less than 3%. Since $\bar{\nu}$ for emulsion is only slightly greater than the $\bar{\nu}$ of chromium, the experimental agreement of the ratios R_{Cr} and R_{emul} supports this conclusion.

C. $D/\langle n_s \rangle$ vs A

It is well known[32] that $D/\langle n_s \rangle$, where $D^2 \equiv \langle (n_s - \langle n_s \rangle)^2 \rangle$, is independent of energy (for $E \gtrsim 50$ GeV) in p-p interactions. Similar behavior is observed in p-emulsion interactions at 67 and 200 GeV.[9] This behavior is a fundamental consequence of KNO scaling.[21-24] A sensitive test for models of hadron-nucleus interactions is their prediction of this quantity as a function of A.

TABLE II. Experimental (see Refs. 9 and 34) and theoretical values for the ratio $D/\langle n_s \rangle$, where $D^2 = \langle n_s^2 \rangle - \langle n_s \rangle^2$.

Target	Experimental	$\eta = 1/3$	$\eta = 1/2$
Proton	0.50 ± 0.01	...	...
Emulsion	0.62 ± 0.01	0.54 ± 0.02	0.60 ± 0.02
Chromium	0.51 ± 0.05	0.51 ± 0.01	0.58 ± 0.01
Tungsten	0.56 ± 0.04	0.53 ± 0.01	0.60 ± 0.01

Using the formula derived by Andersson and Otterlund[33] and a Woods-Saxon calculation of $P_\nu(A)$ (the probability of ν collisions in a nucleus of atomic mass A), we have calculated $D/\langle n_s \rangle$ as a function of A for the CPM and EFC models. In Table II we compare the results of these calculations with the experimental data.[9,34]

The experimental value for emulsion clearly favors the CPM prediction, in agreement with our analysis of R. The chromium and tungsten data of Table II appear to be in agreement with the predictions for $\eta = \frac{1}{3}$ and below those for $\eta = \frac{1}{2}$. However, because of the probable effects, as described below, of biases in the data, we believe that our results are not in disagreement with the $\eta = \frac{1}{2}$ predictions.

The value of $D/\langle n_s \rangle$ is more sensitive than R to a possible scanning bias against the low end of the multiplicity distribution. Since this bias would reduce the value of $D/\langle n_s \rangle$, we believe that the experimental results represent lower limits for this quantity. For example, while an addition of three events of $N_h = 0, n_s = 3$ to the tungsten data would lower R by only half of its statistical error, it would bring the tungsten value for $D/\langle n_s \rangle$ into close agreement with the CPM calculation.

D. Angular distributions

The histograms in Fig. 7 show the pseudorapidity, $r = -\ln \tan(\theta_{\mathrm{lab}}/2)$, distributions of the shower particles emitted from tungsten and chromium targets. We have scaled the distributions for protons on hydrogen[35] from 205 GeV to 300 GeV by displacing the right half of the 205-GeV distribution 0.4 pseudorapidity units to the right. The added area under the curve renormalizes the distribution to the experimentally determined multiplicity at 300 GeV. Also shown are the "excess" pseudorapidity distributions for tungsten and chromium obtained by subtracting the p-p distribution. As noted in several previous papers,[5,6,9,10] for the very forward tracks (large r), the angular distributions for the two metals agree with the

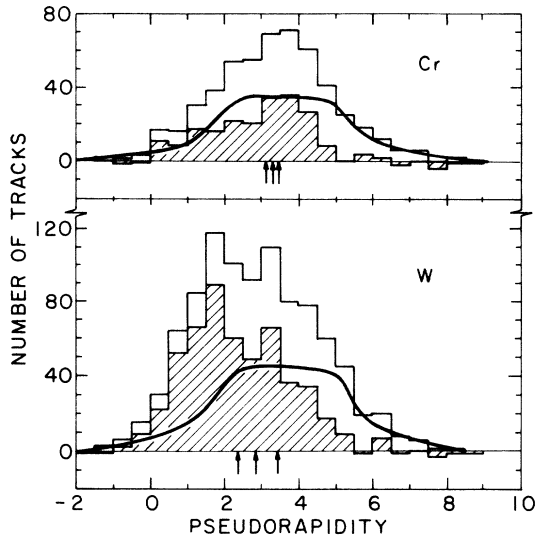

FIG. 7. Pseudorapidity distributions for the chromium and tungsten events. The solid curve represents the 205-GeV hydrogen data scaled to 300 GeV. The shaded histogram shows the distribution of the particles in excess of the hydrogen data. From left to right the arrows indicate the centroids of the excess, metal, and hydrogen distributions.

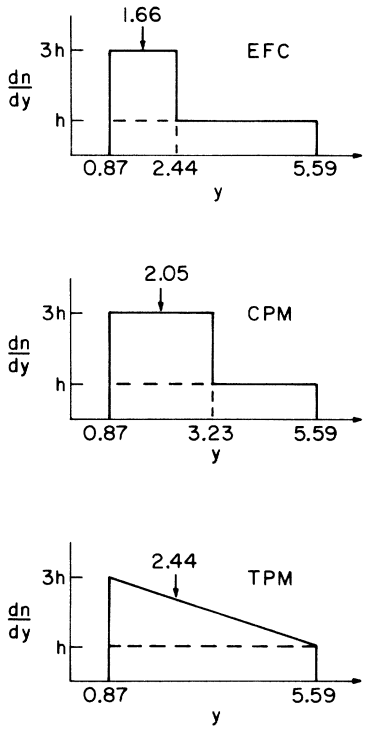

FIG. 8. The predictions of the models for the rapidity distributions assuming a uniform distribution for hydrogen. For illustration, a value of 3 has been assumed for $\bar{\nu}$.

TABLE III. Comparison of model predictions of $\langle r \rangle$ with the experimental values for the tungsten and chromium targets.

Element	EFC	CPM	TPM	Experiment
W	2.76	2.81	3.02	2.83 ± 0.06
Cr	2.96	2.97	3.13	3.32 ± 0.07

p-p distributions. While the excess particles appear at lower pseudorapidities, the excess in chromium peaks at higher pseudorapidity than that in tungsten.

To date, the theories have made only qualitative statements concerning the shape of the excess rapidity distributions. The EFC model predicts that the excess of shower particles is spread uniformly over the backward one-third of the p-p distribution. The CPM prediction has the uniform excess spread over the backward one-half. The TPM prediction has an excess in the shape of a right triangle with no excess in the forward direction and maximum excess in the backward direction. Furthermore, the theories have assumed a rectangular p-p distribution extending to zero rapidity. In order to make more realistic model predictions, we have modified the theories as shown in Fig. 8.

We center the p-p distribution in rapidity at the correct value calculated from the kinematics. This is 3.23 at 300 GeV. The width is set by dividing the p-p multiplicity by the height of the p-p rapidity distribution. We thus use a uniform distribution in rapidity which has a left-hand edge at $y = 0.87$ independent of energy, and which extends to 5.59. This lower limit is a realistic one, corresponding to $\theta \leq 45^\circ$ in the laboratory frame. We then position the cascading excess as indicated by the theories. With these modifications we calculate the centroid of the rapidity spectrum for each of the models. The result is

$$\begin{aligned} &\text{EFC: } \langle y \rangle = 0.87 + 2.36(8 + \bar{\nu}_A)/(6 + 3\bar{\nu}_A), \\ &\text{CPM: } \langle y \rangle = 0.87 + 2.36(3 + \bar{\nu}_A)/(2 + 2\bar{\nu}_A), \\ &\text{TPM: } \langle y \rangle = 0.87 + 4.72(2 + \bar{\nu}_A)/(3 + 3\bar{\nu}_A). \end{aligned} \tag{8}$$

We have done Monte Carlo calculations transforming distributions in rapidity to distributions in pseudorapidity. The result, which is essentially independent of energy, is

$$\langle r \rangle = \langle y \rangle + 0.22 . \tag{9}$$

The resultant centroids in pseudorapidity are displayed in Table III along with the experimental results. While the tungsten value falls within the range predicted by the theories, the chromium result does not.

TABLE IV. Comparison of model predictions of $\langle r \rangle_{\text{excess}}$ with the experimental values for the tungsten and chromium targets.

Element	EFC	CPM	TPM	Experiment
W	1.88	2.27	2.66	2.31 ± 0.11
Cr	1.88	2.27	2.66	3.11 ± 0.18

The theories suggest that the centroid of the excess rapidity distribution should be independent of $\bar{\nu}_A$ and, therefore, independent of A. In Table IV we show that this condition is not met by our data.

Another way to characterize the data is to determine the fraction of the excess particles in the forward one-half of the p-p distribution, that is, with pseudorapidity greater than 3.45. While the EFC and CPM models predict no forward excess, the TPM predicts 25% of the excess to be forward. Our data contain $(36 \pm 5)\%$ of the excess in the forward direction in chromium and $(20 \pm 2)\%$ in tungsten.

The excess pseudorapidity centroids are not very sensitive to our possible scanning bias, since white stars contribute large r values, but have low multiplicities.

V. SUMMARY

The shower particle multiplicity distributions for tungsten and chromium targets are similar to that obtained from a KNO-type scaling of the charged multiplicity distributions in p-p interactions. The multiplicity distributions for the heavily ionizing particles have peaks at around 13 and 8 for tungsten and chromium, respectively. A plot of $\langle n_s \rangle$ vs N_h is linear.

The ratios of the shower particle multiplicity for the metal to that for hydrogen support the prediction $\frac{1}{2} + \frac{1}{2}\bar{\nu}$ obtained from the CPM and TPM and disagree with the Landau and EFC predictions. The value for the dispersion in the multiplicity divided by the average multiplicity is sensitive to possible scanning biases and does not distinguish between the models.

The angular distributions do not agree with the simplified calculations available at present. None of the models predicts the A dependence for the centroid of the distribution in excess of the p-p distribution.

Further progress in this area awaits additional data on elemental targets and more detailed calculations of angular distributions.

ACKNOWLEDGMENTS

We would like to thank Dr. Voyvodic and the Fermilab staff for their help in obtaining the exposure. We would also like to thank D. Sandahl, H. Tepfer, and T. Weber for their help in preparing and scanning the plates and in measuring the events.

*Work supported in part by the U. S. Atomic Energy Commission under Contract No. AT(45-1)-2225.

[1]A. Dar and J. Vary, Phys. Rev. D 6, 2412 (1972).

[2]P. M. Fishbane and J. S. Trefil, Nucl. Phys. B58, 261 (1973); Phys. Rev. Lett. 31, (1973); SUNY Report No. ITP-5B-73-36, 1973 (unpublished); Phys. Rev. D 9, 168 (1974); Phys. Lett. 51B, 139 (1974).

[3]K. Gottfried, Phys. Rev. Lett. 32, 957 (1974).

[4]J. R. Florian, L. D. Kirkpatrick, J. J. Lord, J. Martin, R. E. Gibbs, P. Kotzer, and R. Piserchio, *Particles and Fields—1973*, edited by H. H. Bingham, M. Davier, and G. R. Lynch (A.I.P., New York, 1973).

[5]P. R. Vishwanath, A. E. Bussian, L. W. Jones, D. E. Lyon, Jr., J. G. Learned, D. D. Reeder, and R. J. Wilkes, Phys. Lett. 53B, 479 (1975).

[6]W. Busza, J. E. Elias, D. F. Jacobs, P. A. Swartz, and C. C. Young, Phys. Rev. Lett. 34, 836 (1975).

[7]J. R. Elliott, L. R. Fortney, A. T. Goshaw, J. W. Lamsa, J. S. Loos, W. J. Robertson, Phys. Rev. Lett. 34, 607 (1975).

[8]F. Fumuro, R. Ihara, T. Ogata, and Y. Yukimasa, *Proceedings of the International Cosmic Ray Sumposium on High Energy Phenomena*, 179, 1974 (unpublished).

[9]J. Babecki, J. Z. Czachowska, B. Furmanska, J. Gierula, R. Holynski, A. Jurak, S. Krzywszinski, G. Nowak, B. Slezak, and W. Wolter, Phys. Lett. 47B, 268 (1973).

[10]J. Hêbert *et al.*, Barcelona-Batavia-Belgrade-Bucharest-Lund-Lyon-McGill-Nancy-Ottawa-Paris-Quebec-Rome-Valencia Collaboration, in *Experiment on High Energy Particle Collisions—1973*, proceedings of the International Conference on New Results from Experiments on High Energy Particle Collisions, Vanderbilt University, edited by Robert S. Panvini (A.I.P., New York, 1973); *High Energy Physics and Nuclear Structure, Proceedings of the Fifth International Conference on High Energy Physics and Nuclear Structure, Uppsala, Sweden, 1973*, edited by G. Tibell (North-Holland, Amsterdam, 1974).

[11]J. I. Cohen, E. M. Friedlander, M. Marcu, A. A. Martin, and R. Nitu, Nuovo Cimento Lett. 9, 337 (1974).

[12]S. Z. Belenkij and L. D. Landau, Nuovo Cimento Suppl. 3, 15 (1956).

[13]P. M. Fishbane and J. S. Trefil, Phys. Rev. D 9, 168 (1974).

[14]P. M. Fishbane and J. S. Trefil, Phys. Lett. 51B, 139

(1974).
[15]We wish to thank W. Busza for bringing this relationship to our attention.
[16]S. P. Denisov, S. V. Donskov, Yu. P. Gorin, R. N. Krasnokutsky, A. I. Petrukhin, Yu. D. Prokoshkin, and D. A. Stoyanova, Nucl. Phys. B61, 62 (1973).
[17]P. J. Camillo, P. M. Fishbane, and J. S. Trefil, 1974 (private communication).
[18]R. J. Glauber, in *High Energy Physics and Nuclear Structure*, proceedings of the Second International Conference, Rehovoth, Israel, 1967, edited by G. Alexander (North-Holland, Amsterdam, 1967), p. 311.
[19]C. F. Powell, P. H. Fowler, and D. H. Perkins, *The Study of Elementary Particles by the Photographic Method* (Pergamon, New York, 1959), p. 571.
[20]J. Lach and S. Pruss, Fermilab Technical Memo No. TM-285/2254.000 (unpublished).
[21]P. Slattery, Phys. Rev. Lett. 29, 1624 (1972); Phys. Rev. D 7, 2073 (1973).
[22]P. Olesen, Phys. Lett. 41B, 602 (1972).
[23]Z. Koba, H. B. Nielsen, and P. Olesen, Nucl. Phys. B40, 317 (1972).
[24]J. W. Martin, J. R. Florian, L. D. Kirkpatrick, J. J. Lord, and R. E. Gibbs, Nuovo Cimento 25A, 447 (1975).
[25]A. Gurtu *et al.*, Phys. Lett. 50B, 391 (1974).
[26]R. E. Gibbs, J. R. Florian, L. D. Kirkpatrick, J. J. Lord, and J. W. Martin, Phys. Rev. D 10, 783 (1974).
[27]H. Meyer, M. W. Teucher, and E. Lohrmann, Nuovo Cimento 28, 1399 (1963).
[28]S. Kaufman, Phys. Rev. 129, 1866 (1963).
[29]R. E. Gibbs, J. J. Lord, and E. R. Goza, in *Proceedings of the Sixth InterAmerican Seminar on Cosmic Rays*, La Paz, Bolivia, 1970 (Universidad Mayor de San Andres, La Paz, 1070), Vol. 3, p. 639.
[30]B. Furmanska and B. Slezak, 1973 (private communication).
[31]I. Otterlund, University of Lund Report No. LUIP-CR-74-12, 1974 (unpublished).
[32]F. T. Dao, J. Lach, and J. Whitmore, Phys. Lett. 45B, 513 (1973).
[33]B. Andersson and I. Otterlund, Nucl. Phys. B88, 349 (1975).
[34]A. Firestone *et al.*, Phys. Rev. D 10, 2080 (1974).
[35]G. Charlton *et al.*, Phys. Rev. Lett. 29, 515 (1972).